# A CAD Tool for the Design and Optimization of Schottky Diode Mixers up to Terahertz Frequencies

José V. Siles and Jesús Grajal
Dept. Señales, Sistemas y Radiocomunicaciones
E.T.S.I.T., Universidad Politécnica de Madrid
Ciudad Universitaria s/n, E-28040 Madrid, Spain
Email: {jovi, jesus}@gmr.ssr.upm.es
Telephone: +34 913367358
Fax: +34 913367362

Viktor Krozer
Orsted-DTU
Technical University of Denmark
Orsted Plads, building 348
DK-2800 Kgs. Lyngby, Denmark

Bruno Leone
European Space Agency
ESA/ESTEC
Keplerlaan, Noordwijk
The Netherlands

***Abstract*— Emerging applications at millimeter and submillimeter-wave spectral bands demand reliable CAD tools to be employed in the design of receivers up to Terahertz frequencies. In this paper we present a CAD tool for the design and optimization of Schottky diode frequency mixers at millimeter and submillimeter-wave spectral bands. This tool couples a diode physical numerical model with the circuit simulator using a multi-tone harmonic balance technique based on the *Almost Periodic Fourier Transform* (APFT). Contrary to approximate approaches, as matrix conversion techniques, no restrictions are considered regarding LO and RF pump powers. The mixer CAD tool allows a complete analysis of mixer circuits up to Thz frequencies taking into account both the external circuit and the Schottky diode structure.**

## I. Introduction

Terahertz spectral bands are one of the least explored regions of the electromagnetic spectrum with applications in radio-astronomy, planetary science, security, medicine, etc. The necessity for Terahertz circuit development makes essential to have accurate simulation tools to be employed in the design and optimization of these circuits as a previous step to the fabrication process [1].

In this paper we present a novel CAD tool that couples a Schottky diode physical numerical model with a circuit simulator using appropriate harmonic-balance techniques (Fig. 1). This allows the concurrent design of circuits (mixers, detectors and multipliers) taking into account both the device structure (doping and length of the epitaxial layer, and area of the device) and the embedding circuit (bias, available power, and loads at different harmonics and intermodulation frequencies). A similar CAD for Schottky multipliers design was already presented in [2], [3], [4].

The Schottky diode model consists of a physics-based numerical device simulator which incorporates accurate boundary and interface conditions for self-consistent treatment of tunnelling transport, image-force effects, impact ionization, and non-constant recombination velocity. This physics-based simulator accounts for limiting mechanisms such as avalanche breakdown, velocity saturation, and increase in the series resistance with the input power.

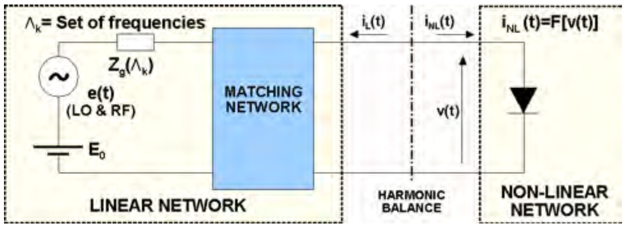


Fig. 1. Schematic of the analyzed circuit for mixers simulation.

Commercial programmes are based on approximate approaches, as conversion matrix techniques. Our general-purpose mixer CAD tool takes into account not only LO and RF harmonics but also their intermodulation products, with no restrictions regarding LO and RF pump powers. Thus, a complete mixer design and full optimization task can be performed with this tool up to Terahertz frequencies. All mixer parameters can be taken into account during the optimization (LO and RF power, impedances at every frequency, etc.).

Mixer analysis requires a proper selection of the time-frequency conversion technique if a general-purpose mixer simulator is required. Several techniques have been studied: Discrete Fourier Transform (DFT), Multidimensional Discrete Fourier Transform (MDFT) and Almost Periodic Fourier Transform (APFT). As a conclusion, APFT has been finally selected. It supports non-commensurable frequencies and can be applied to numerical models non-defined by algebraic equations (in contrast to MDFT).

## II. Techniques for Multi-tone Harmonic Balance

There are different methods available for transforming signals between time and frequency domains that are suitable for use with multi-tone signals. The most important are:

- **FFT (*Fast Fourier Transform*):** Only applicable to mixer analysis when LO and RF frequencies are commensurable. In this case, a base frequency for the FFT can be selected as the great common divider of LO and RF.

- **MFFT (*Multidimensional Fast Fourier Transform*):** A generalization of the FFT to analyze circuits whose base frequencies are incommensurable. It is the most general algorithm with no additional assumptions to the ones assumed for the traditional harmonic balance for periodic signals, but it requires models described by algrebraic equations [5].
- **APFT *(Almost Periodic Fourier Transform):*** APFT is based on a generalization of the matrix form of the Fourier transform without any restriction regarding the frequencies to be analyzed and the sampling instants. These approaches are slower than MFFT and mapping techniques because APFTs do not employ the FFT. However, APFTs support incommensurable frequencies and are easy to implement and very flexible.
- **Mapping Techniques:** Actual base frequencies are replaced by artificially selected base frequencies, so that the original spectrum is mapped onto an equivalent periodic and dense spectrum. Waveforms transformed through the mapping become periodic and its Fourier coefficients can be efficiently calculated by the one-dimensional FFT.

Aspects such as underlying assumptions, limitations, flexibility, dynamic range and time consumption in the calculations have been considered before selecting the algorithms to be implemented in the simulator. After an in-depth study of the different approaches, the most appropriate algorithm are the APFTs. This is because *MFFT* and *Mapping Techniques* are only valid for non-linear systems described by algebraic relationships, i.e., memoryless systems. FFT does not support incommensurable frequencies and the computational cost highly depends on $gcd(f_{LO}, f_{RF})$.

### A. Introduction to the APFT

APFT is based on a generalization of the matrix form of the Fourier transform without any restriction regarding the frequencies to be analyzed and the sampling instants.

By considering only a finite number of frequencies $\Delta_K = \{w_0,\ w_2,\ ...,\ w_{K-1}\}$, it is possible to sample a waveform at a finite number of time points and calculate its Fourier coefficients.

If $X(k) = X_k^C + j \cdot X_k^S$ represents the Fourier coefficients at frequencies $w_k$ of a certain waveform $x(t)$, and assuming a certain truncation error, $x(t)$ can be expressed as:

$$x(t) = \sum_{w_k \in \Lambda_k} \left( X_k^C \cdot \cos(w_k \cdot t) + X_k^S \cdot \sin(w_k \cdot t) \right) \quad (1)$$

By sampling $x(t)$ at S time points, Eq. 1 can be rewritten as a matrix product,

$$x = A \cdot X \quad (2)$$

where,

$$x = [x(t_1)\ x(t_2)\ x(t_3)\ ...\ x(t_S)]^T \quad (3)$$

$$X = \left[ X_0\ X_1^C\ X_1^S\ ...\ X_{K-1}^C\ X_{K-1}^C \right]^T \quad (4)$$

$$A = \begin{bmatrix} 1 & \cos(w_1 t_1) & \sin(w_1 t_1) & ... & \cos(w_{K-1} t_1) & \sin(w_{K-1} t_1) \\ 1 & \cos(w_1 t_2) & \sin(w_1 t_2) & ... & \cos(w_{K-1} t_2) & \sin(w_{K-1} t_2) \\ 1 & \cos(w_1 t_3) & \sin(w_1 t_3) & ... & \cos(w_{K-1} t_3) & \sin(w_{K-1} t_3) \\ . & . & . & & . & . \\ . & . & . & & . & . \\ . & . & . & & . & . \\ 1 & \cos(w_1 t_s) & \sin(w_1 t_s) & ... & \cos(w_{K-1} t_s) & \sin(w_{K-1} t_s) \end{bmatrix} \quad (5)$$

Fig. 2 shows a general flowchart for APFT methods, including the three steps mentioned above.

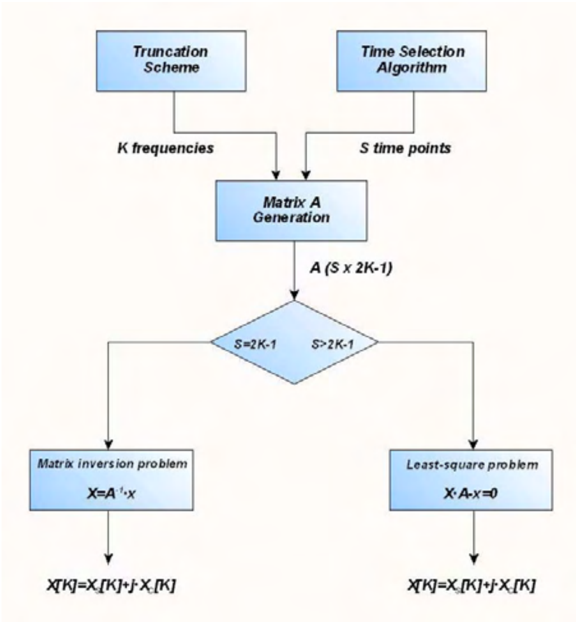


Fig. 2. General flowchart of APFT techniques.

The accuracy on the estimation of Fourier coefficients with the APFT is determined by two factors. On the one hand, the aliasing error due to omitting frequencies in the transform is reduced by increasing the number of components in the frequency set $\Lambda_k$ (truncation scheme in Fig. 2). On the other hand, assuming a certain discretization error in the time domain waveforms, a numerical error will be present in the Fourier coefficients, which will be given by,

$$\frac{\|\Delta X\|}{\|X\|} \leq \kappa(A) \cdot \frac{\|\Delta x\|}{\|x\|} \quad (6)$$

where $\kappa(A) = \|A\| \cdot \|A^{-1}\|$ is the condition number of matrix $A$ and $\| \cdot \|$ represents the norm of a matrix in a certain metric space. Usually 2-norm, $\infty - norm$ and Frobenius norm are employed.

To reduce the error, the condition number must be minimized, and this occurs when columns in matrix A becomes near-orthogonal.

Initial approaches to the APFT consisted of an uniform or random selection of the minimum necessary time points ($S = 2K - 1$) to form an square matrix $A$, which was in general extremely ill-conditioned leading to bad APFT results. Kundert and Sorkin [6] proposed in 1988 a time-selection algorithm to choose an adequate set of time points in order to guarantee a well-conditioned square matrix A. In this case, the time-selection algorithm can be seen as an orthogonalization process. The vector $X$ of Fourier coefficients can be directly calculated just by computing the ordinary inverse of $A$, and yields Eq. 7.

$$X = A^{-1} \cdot x \tag{7}$$

If A is not an square matrix, that is $S > 2K - 1$, the problem of computing Fourier coefficients consists of finding the shortest vector $X$ that minimizes the distance $\rho(X)$ (Eq. 8). This is a typical least-square problem that can be solved by methods published in literature: [7] - [10]. This APFT scheme was firstly suggested by Zhang and Hong in 1990 [11]. Another time-selection algorithm, different from the one employed in [6] was applied to obtain $S$ time points 2 or 3 times the $2K-1$ points required. By combining the orthogonalization in the time-selection algorithm with the solving of the overdetermined system by least-squares accuracy is improved with respect to previous methods.

$$\rho(X) = \|x - A \cdot X\| \tag{8}$$

Other implementations of the APFT have been published since [11]. The orthogonal APFT by Rodrigues [12] achieves the best possible conditioning for matrix A by making it exactly orthogonal. Unfortunately, this method has a big inconvenient when applied to device models that are not described by analytical equations. This inconvenient is related to the highest time instant $t_{max}$ where the time domain waveform must be evaluated, which in Rodrigues' APFT depends on the desired significant digits to be taken into account for representing the frequency values in the analysis. As the numerical model of the Schottky diode is described by partial differential equations, and considering that a high sampling frequency (low time steps) is mandatory to reduce the error in the time domain resolution of such a system, then a high number of points would be necessary to reach the mentioned $t_{max}$.

## *B. APFT implementation in the mixers CAD tool*

To summarize, a good APFT method should solve two important problems. First, the need for accuracy in the estimation of Fourier coefficients, which is directly proportional to the condition number of matrix $A$. Second, the computation time that is required, which depends not only on the number of frequencies and the number of time points to be considered but also on the time-selection algorithm. Thus, for the mixers CAD tool we have implemented an APFT method, conceptually similar to the one by Zhang and Hong but with the following simplifications and considerations:

- The time-selection algorithm is simplified to a random selection of $S$ time-points. As a consequence, a poor-conditioned matrix $A$ is generated .
- Fourier coefficients vector $X$ is estimated by $X = A^I x$, where $A^I$ is the Moore-Penrose pseudo-inverse of matrix A (also known as generalized inverse) [9]. The motivation for employing pseudo-inverse lies on the fact that this method proportionates the solution that minimizes the distance given by Eq. 6. In [7] it is discussed the strategy of using the Moore-Penrose generalized inverse to solve poorly-conditioned systems.

Table I shows a comparison between several APFTs and the one we have proposed and employed in the multi-tone harmonic balance tool for mixer analysis. The test has been performed by applying the APFT to the time domain current signal obtained by pumping a Schottky diode with a 2-tone ($P_{LO}$=2 mW @ 100 GHz and $P_{RF}$=0.1 mW @ 105 GHz) voltage waveform. A *box* truncation scheme (box $H_1 X H_2$) has been employed, where $H_1$ and $H_2$ indicate that only those frequency components corresponding to $H_1$ LO harmonics, $H_2$ RF harmonics and their intermodulation products have been taking into account. $M$ is the number of points employed in the time-selection algorithms to choose the $S$ points that will be used to form matrix $A$

The random component inherent to the time points selection in APFT techniques makes necessary to perform a Monte Carlo analysis in order to evaluate the statistical goodness of the results. An unbiased estimation of conversion loss (taking as reference the results obtained by the FFT) together with a low standard deviation are desired. Results are shown in table I), where $E[L]$ represents the mean conversion loss and $\sigma_L$ is the standard deviation.

Computation times correspond to a single execution of the APFT. The Monte Carlo analysis has been done using *Mathworks MATLAB 7.0* running on a Pentium IV platform with a 2.8 GHz clock frequency and 1 GB of available RAM.

TABLE I
COMPUTATION TIME AND ACCURACY OF APFT TECHNIQUES

| | | | | Kundert-Sorkin's APFT | | | Zhang-Hong's APFT | | | Proposed APFT | | |
|---|---|---|---|---|---|---|---|---|---|---|---|---|
| Truncation | k | N=2k-1 | M | E[L] (dB) | $\sigma_L$ (dB) | Time (s) | E[L] (dB) | $\sigma_L$ (dB) | Time (s) | E[L] (dB) | $\sigma_L$ (dB) | Time (sec) |
| Box 2X2 | 13 | 25 | 2·N | 5.82 | 5.18 | **0.890** | 6.86 | 4.60 | **0.735** | 7.60 | 4.63 | **0.890** |
| | | | 5·N | 8.20 | 4.31 | **1.880** | 6.91 | 2.89 | **1.080** | 7.52 | 3.30 | **1.265** |
| | | | 8·N | 7.42 | 4.64 | **1.516** | 7.11 | 1.69 | **1.719** | 6.88 | 1.80 | **1.625** |
| Box 4X4 | 41 | 81 | 2·N | 6.98 | 2.57 | **3.109** | 6.92 | 0.97 | **6.110** | 6.63 | 0.81 | **3.172** |
| | | | 5·N | 6.75 | 0.43 | **6.954** | 6.71 | 0.24 | **43.703** | 6.72 | 0.27 | **7.203** |
| | | | 8·N | 6.77 | 0.36 | **10.781** | 6.68 | 0.15 | **124.390** | 6.69 | 0.18 | **11.203** |
| Box 6X6 | 85 | 169 | 5·N | 6.68 | 0.16 | **31.578** | 6.70 | 0.03 | **1002.125** | 6.70 | 0.03 | **32.422** |

Fig. 3 shows the influence of the truncation on the accuracy of APFT methods. Results have been compared with those obtained by FFT that is the technique that proportionates the best accuracy because it is the best conditioned and consequently it is much less influenced by the aliasing error. Notice that APFT results tend to FFT results with an accuracy better than 0.2 dB when a *Box 4X4* truncation or higher is selected. It is also important to have in mind that the computation of the pseudo-inverse of $A$ is only performed once at the beginning of the simulation process, and there is no need to recalculate it during the analysis.

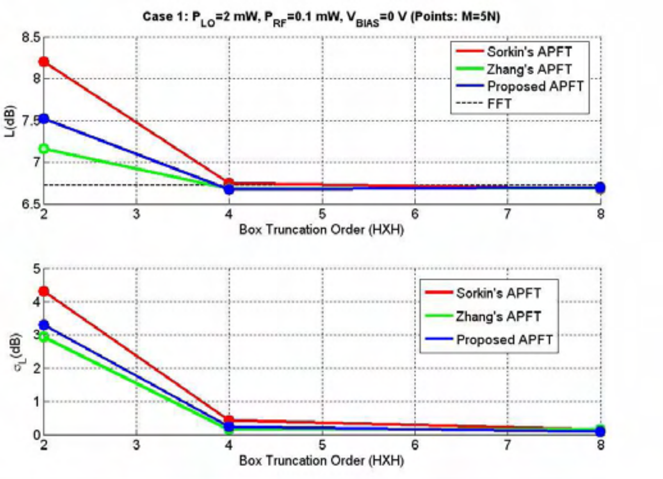


Fig. 3. Influence of truncation on APFT performance

## III. Mixers Design and Optimization

It has been already commented that our CAD tool allows the concurrent analysis and optimization of the external circuit and the Schottky diode. In this section we present how the different design parameters affect to the performance of the mixer circuit.

### A. External circuit parameters

In contrast to multiplier design, mixers are limited less by the properties of the Schottky diode than by those of the circuit, especially the practical impossibility of achieving optimum terminations at a large number of mixing frequencies. Some ways to optimize the external circuit are the use of DC bias, optimization of LO power, image enhancement, and the use of matched source and load impedances [13]. Of course, IF impedance must be also optimized to minimize conversion loss. In the CAD tool, this task is done by an optimization algorithm based on the gradient descent method.

As can be seen in Fig. 4, there is a trade-off between LO power and bias [13]. Furthermore, conversion loss is minimized and gets constant beyond a certain LO power, consequently, there is a linear relationship between IF and LO powers. Fig. 5 shows the variation in the real part of the conjugate-matched LO impedance as a function of LO power. As in multipliers [3], $Re[Z(f_{LO})]$ increases with bias as a consequence of the higher electric fields inside the Schottky diode that reduce the electron mobility.
The sensitivity of conversion loss with IF impedance is analyzed in Fig 6. It can be depicted that the IF impedance is not a limiting factor due to the wide range of values where minimum loss are achieved.

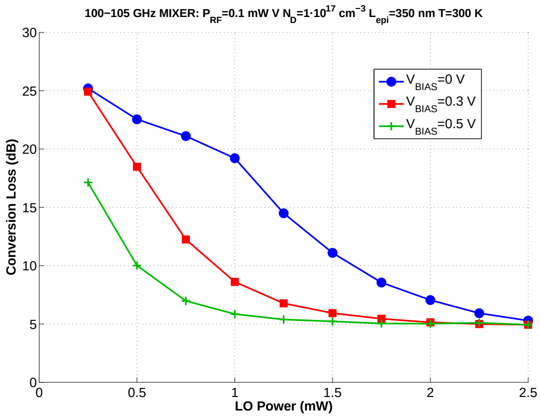


Fig. 4. 100-105 GHz Mixer. Influence of DC bias on conversion loss

One of the best known methods of reducing the conversion loss of a mixer is to terminate the diode in a reactance at the image frequency. Thus, power that would be dissipated in the image termination is converted to the IF [13]. It can be noticed in Fig 7 the reduction of the conversion loss through a correct choice of the image terminating reactance in the 100-105 GHz mixer circuit. Although the minimum conversion loss occurs for a $50\Omega$ reactance, it is convenient to choose a higher value for it in order to avoid the high sensitivity region.

Another well-known characteristic of mixers performance is illustrated in Fig. 8. When the RF power is much lower than the LO power, which is the general regime in space applications receivers, conversion loss are determined by LO power and the influence of RF power can be neglected. This is the fundamental assumption of

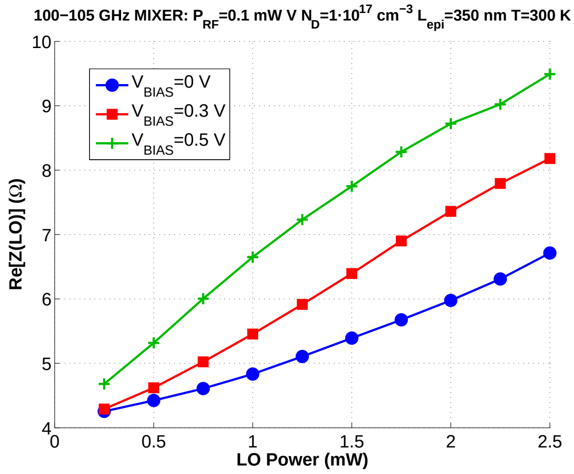


Fig. 5. 100-105 GHz Mixer. Influence of DC bias on matched $Re[Z(f_{LO})]$

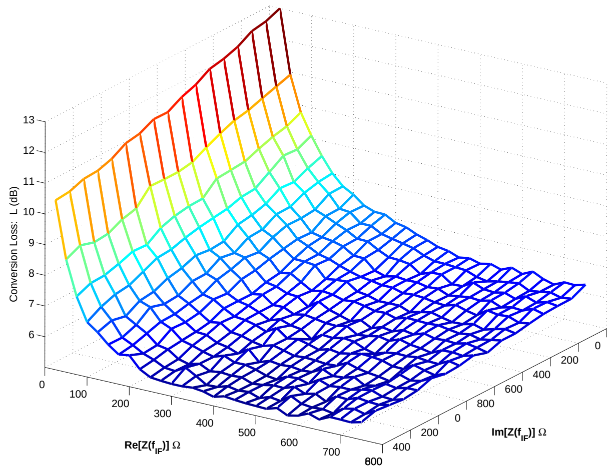


Fig. 6. 100-105 GHz Mixer. Influence of IF impedance on conversion loss. $P_{LO} = 2$ mW

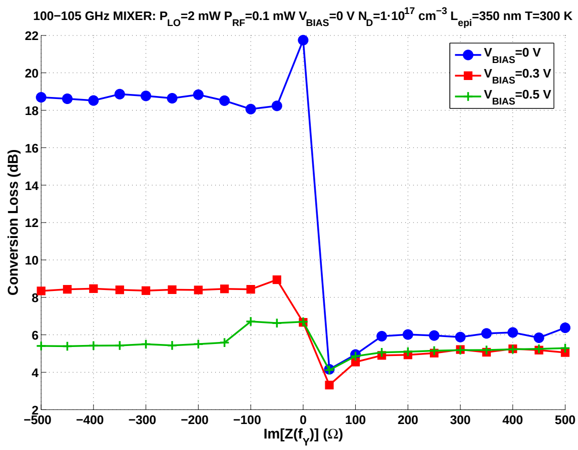


Fig. 7. 100-105 GHz Mixer. Image Enhancement

those simulators based on approximate approaches as the impedance matrix conversion techniques. Fig. 8 also demonstrates that our mixer CAD tool allows the analysis of mixers when they are operating well into the non-linear region for RF.

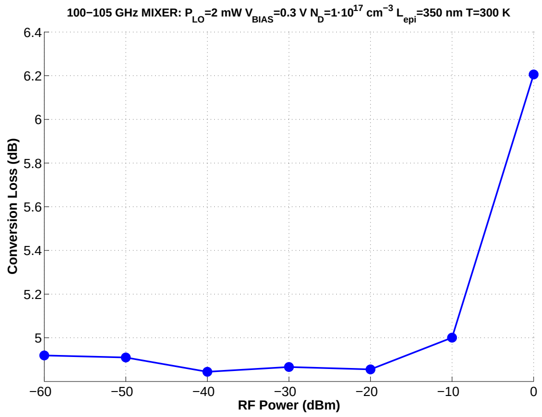


Fig. 8. 100-105 GHz Mixer. Influence of RF power on conversion loss. $P_{LO}$=3 dBm

## B. Schottky diode parameters

The influence on performance of the Schottky diode parameters (anode are, epilayer length and doping, temperature, ...) is analogous to the multipliers performance (see [2]). For instance, as it occurs in multipliers, dividing by 2 the anode area of the Schottky diode, the curve of conversion loss shifts 3 dBm to the left so minimum losses can be achieved with half LO power (Fig. 9). Fig. 10 shows the reduction in conversion loss when the length of the epitaxial layer is reduced, as a consequence of a lower series resistance.

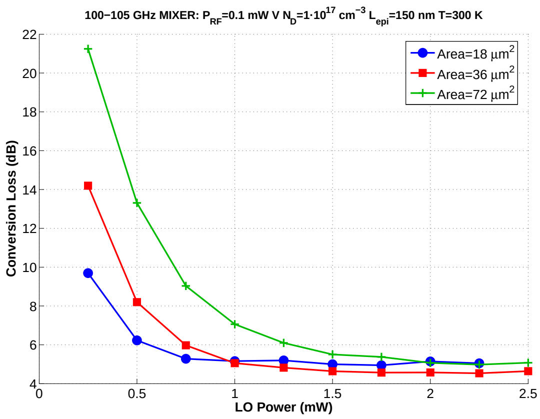


Fig. 9. 100-105 GHz Mixer. Influence of anode area on conversion loss

Influence of ambient temperature (self-heating has not been considered) in the mixer performance is also presented in Fig. 12. Conversion loss is reduced as a consequence of higher electron mobilities at low temperatures.

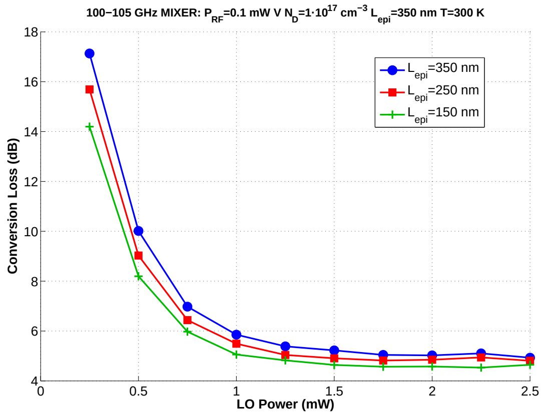


Fig. 10. 100-105 GHz Mixer. Influence of epilayer length on conversion loss

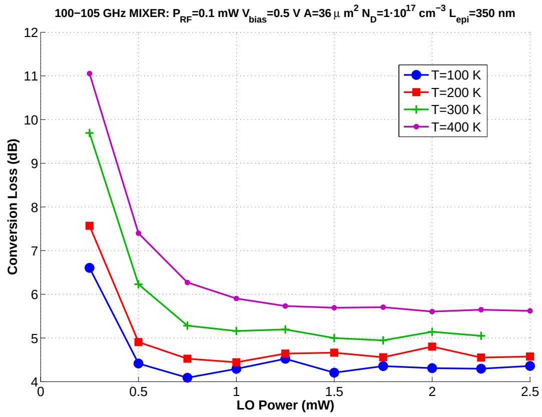


Fig. 11. 100-105 GHz Mixer. Influence of temperature on conversion loss

## IV. Validation

The validation of the numerical simulator for mixers design, as for multipliers, requires a great quantity of data from Schottky mixer measurements. Unfortunately, only a few data have been published in literature [14] - [20], which is not enough to afford a complete validation of the simulation tool. Anyway, the numerical simulator was already validated for multipliers design and this can be extended to the mixer design just by taking into account that the only change in the simulator lies on the time-frequency conversion techniques that are employed.

Fig 12 shows simulation results for the 585 GHz mixer described in [18]. A conversion loss of 8 dB, achieved in the range of 0.2 to 1 mW LO power is reported for this mixer. According to harmonic balance simulations, the 8 dB conversion loss is obtained at around 0.6 mW of LO power. Since no information is given in [18] regarding the termination impedances at the image frequency, three cases have been simulated: $Z_Y = 50\Omega$, $Z_Y = Z_{LO,matched}$ and $Z_Y = 0+j300$ $\Omega$ (image enhancement).

A 100 GHz mixer has been also simulated with similar parameters to those corresponding to the mixer circuit reported in [14]. The conversion loss (5.3 dB) is analogous to the obtained by the numeric mixer CAD tool.

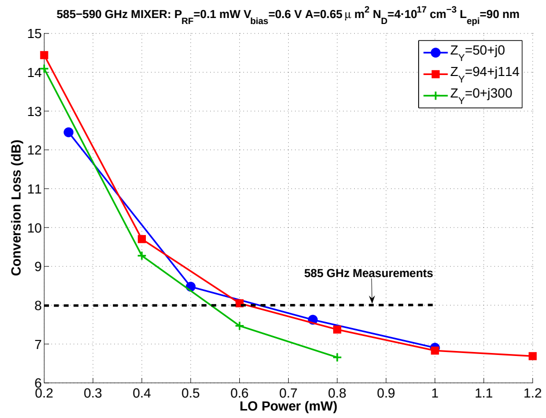


Fig. 12. Simulated conversion loss for the 585 GHz mixer described in [18]

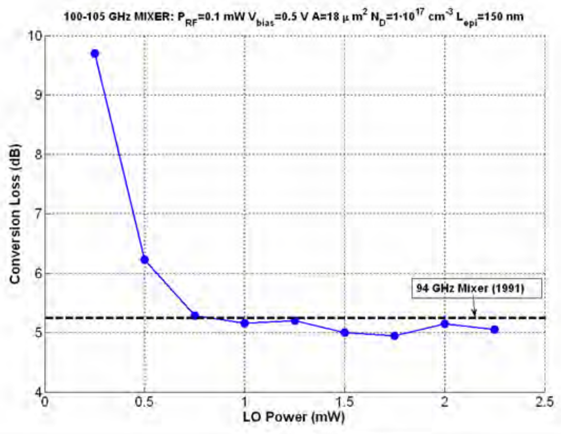


Fig. 13. Simulated conversion loss for the 94GHz mixer described in [14]

## V. CONCLUSION

A novel CAD tool has been presented for the design and optimization of mixer circuits at millimeter and submillimeter-wave bands. One of the advantages of this tool is that no assumptions are made regarding LO and RF powers and frequencies. The mixer CAD tool represents a complement to a previous existent simulation tool for multipliers. As a result, a complete simulation tool is available for the design of receivers up to Terahertz frequencies.

The degree of freedom that arises as a consequence of the coupling of a numerical model for Schottky diodes with the harmonic balance circuit simulator has enabled us to study the different operation regimes and the physical limitations of mixers from the circuit point of view: bias, input power, loads at different frequency components, etc.

Mixer design and optimization aspects have been presented, which show the potential of the CAD tool to perform different analysis of mixer circuits taking into account all possible design parameters. Some comparisons between simulations and measurements have been presented. Further efforts to validate the mixer CAD tool are in progress.

## ACKNOWLEDGMENT

The authors would like to thank the partial financial support of the European Space Agency to this work, under contract GSTP-3 ref. RIDER1 15293/01/NL/NF.

## REFERENCES


[1] P. H. Siegel, “Terahertz technology,” *IEEE Transactions on microwave theory and techniques*, vol. 50, pp. 910–928, March 2002.
[2] J. Grajal, V. Krozer, E. Gonzalez, F. Maldonado, and J. Gismero, “Modelling and design aspects of millimeter-wave and submillimeter-wave Schottky diode varactor frequency multipliers,” *IEEE Transactions on microwave theory and techniques*, vol. 48, pp. 910–928, April 2000.
[3] J. Grajal, J. Siles, V. Krozer, E. Sbarra, and B. Leone, “Analysis and design of schottky diode multiplier chains up to Terahertz frequencies,” *In Proc. ESA Microwave Technology Techniques Workshop: Preparing for Future Space Systems*, May 2004.
[4] J. Grajal, J. Siles, V. Krozer, E. Sbarra, and B. Leone, “Performance evaluation of multiplication chains up to THz frequencies,” *In Proc. 29th International Conference on Infrarred and Millimeter Waves 12th International Conference on Terahertz Electronics*, September 2004.
[5] P. Heron and M. Steer, “Jacobian calculation using the Multidimensional Fast Fourier Transform in the harmonic balance analysis of nonlinear circuits,” *IEEE Transactions on Microwave Theory and Techniques*, vol. 38, no. 4, pp. 429–431, 1990.
[6] K.S.Kundert, G. Sorkin, and A. Sangiovanni-Vincentelli, “Applying harmonic balance to almost-periodic circuits,” *IEEE Transactions on Microwave Theory and Techniques*, vol. 36, no. 2, pp. 366–378, 1988.
[7] G. Golub and C. Loan, *Matrix Computations (2nd Edition)*. John Hopkins University Press, 1989.
[8] A. Bjorck, *Least squares methods: Handbook of numerical analysis Vol. 1. Solution of equations in $N$*. Elsevier North Holland, 1988.
[9] R. Penrose, “A generalized inverse of matrices,” *Proc. Cambridge Philos. Soc. 51*, 1954.
[10] B. Rust, W. Burrus, and C.Schneeberger, “A simple algorithm for computing the generalized inverse of a matrix,” *Communications of the ACM*, vol. 9, pp. 381–387, 1966.
[11] X.-D. Zhang, X.-N. Hong, and B.-X. Gao, “An accurate fourier transform method for nonlinear circuits analysis with multi-tone driven,” *IEEE Transactions on Circuits and Systems*, vol. 37, no. 5, pp. 668–669, 1990.
[12] P. J. Rodrigues, *Computer-aided analysis of nonlinear microwave circuits*. Artech-House, Inc. Boston-London, 1997.
[13] S. Maas, *Microwave Mixers (Second edition)*. Artech-House, Inc. Boston-London, 1986.
[14] D. Garfield, R. Mattauch, and S. Weinreb, “RF performance of a novel planar millimeter-wave diode incorporating an etched surface channel,” *IEEE Transactions on Microwave Theory and Techniques*, vol. 39, pp. 1–5, January 1991.
[15] A. Kerr, R. Mattauch, and J. Grange, “A new mixer design for 140-220 GHz,” *IEEE Transactions on Microwave Theory and Techniques*, pp. 399–401, May 1977.
[16] P. Siegel and A. Kerr, “The measured and computed performance of a 140-220 GHz schottky diode mixer,” *IEEE Transactions on Microwave Theory and Techniques*, vol. 32, pp. 1579–1590, December 1984.
[17] T. Newman and K. Ng, “A submillimeter-wave planar diode mixer design and evaluation,” *IEEE MTT-S Digest*, pp. 1293–1296, 1991.
[18] K. Hui, J. Hesler, D. Kurtz, W. Bishop, and T. Crowe, “A micromachined 585 GHz Schottky mixer,” *IEEE Microwave and Guided Wave Letters*, vol. 10, pp. 374–376, September 2000.
[19] P. Siegel, I. Mehdi, R. Dengler, T. Lee, D. Humphrey, and A. Pease, “A 640 GHz planar-diode fundamental mixer/receiver,” *IEEE MTT-S Digest*, pp. 407–410, 1998.
[20] S. Gearhart, J. Hesler, W. Bishop, T. Crowe, and G. Rebeiz, “A wide-band 760 GHz planar integrated schottky receiver,” *IEEE Microwave and Guided Wave Letters*, vol. 3, pp. 205–207, July 1993.